18F-Sodium Fluoride Positron Emission Tomography/Computed Tomography in Ex Vivo Human Coronary Arteries With Histological Correlation

Arteriosclerosis, Thrombosis, and Vascular Biology

TRANSLATIONAL SCIENCES

^{18}F-Sodium Fluoride Positron Emission Tomography/Computed Tomography in Ex Vivo Human Coronary Arteries With Histological Correlation

Trisha Youn, Subhi J. Al'Aref, Navneet Narula, Steven Salvatore, David Pisapia, Marc R. Dweck, Jagat Narula, Fay Y. Lin, Yao Lu, Amit Kumar, Renu Virmani, James K. Min

OBJECTIVE: ^{18}F-sodium fluoride (NaF) position emission tomography (PET) activity correlates with high-risk plaque. We examined the correlation between ^{18}F-NaF PET activity and extent of calcification (microcalcification and macrocalcification) in coronary arteries.

APPROACH AND RESULTS: Eighteen ex vivo human coronary arteries were imaged with ^{18}F-NaF PET/CT, and target to background ratios were analyzed from 101 plaques. Histopathologic analysis evaluated for microcalcification and macrocalcification, plaque morphology, and inflammation. Plaques with microcalcification demonstrated higher ^{18}F-NaF PET activity (n=84; mean target to background ratio±SD, 9.0±9.7,) than plaques without microcalcification (n=17, 2.9±3.8; $P<0.0001$). Higher ^{18}F-NaF PET activity was associated with advanced plaques characterized by fibroatheroma (n=54, 10.7±10.3) compared with plaques with intimal thickening (n=22, 3.5±3.9) or pathological intimal thickening (n=25, 6.1±8.4; $P=0.004$). No significant association was found between ^{18}F-NaF PET activity and inflammation ($P=0.08$).

CONCLUSIONS: In ex vivo human coronary arteries, higher ^{18}F-NaF PET activity was associated with microcalcification and advanced plaque morphology. Since microcalcification and fibroatheromas are high-risk plaque features, ^{18}F-NaF PET/CT may improve risk-stratification.

VISUAL OVERVIEW: An online visual overview is available for this article.

Key Words: atherosclerotic plaque ■ calcification ■ computed tomography angiography ■ inflammation ■ risk factor

Prediction of future adverse events in coronary heart disease remains challenging.[1] Identification of high-risk plaque precursors for myocardial infarction is one potential strategy for individualized assessment of cardiovascular risk. Characteristics of high-risk plaque on noninvasive imaging, such as computed tomography (CT) angiography, include the presence of low attenuation plaque, positive arterial remodeling, and microcalcification.[2,3] Also, while the presence of macrocalcification is generally associated with healed and stable plaque, the presence of microcalcification is, by contrast, a hallmark of unstable plaque.[4] Macrocalcification can be readily detected by conventional CT imaging, while the presence of microcalcification can be challenging to assess due to spatial resolution constraints.[5,6]

^{18}F-sodium fluoride (NaF) is a radiotracer that preferentially identifies microcalcification in arteries by binding to hydroxyapatite.[4,7–9] ^{18}F-NaF positron emission tomography (PET) activity also co-localizes to high-risk and culprit coronary plaque and is currently being investigated as a prognostic marker in the large multicenter PREFFIR study (Prediction of Recurrent Events With 18F-Fluoride). Studies have been performed in carotid artery specimens correlating ^{18}F-NaF activity with microcalcification.[10] However, within the coronary arteries, the histopathologic correlation of vulnerable plaque features such as microcalcification,

Correspondence to: Trisha Youn, MD, Department of Radiology, Weill Cornell Medicine, 520 E 70th St, Starr Pavilion 2nd Floor, New York, NY 10021. Email yhy111@gmail.com

This article was sent to Zahi Fayad, Consulting Editor, for review by expert referees, editorial decision, and final disposition.

The online-only Data Supplement is available with this article at https://www.ahajournals.org/doi/suppl/10.1161/ATVBAHA.119.312737.

For Sources of Funding and Disclosures, see page 411.

Arterioscler Thromb Vasc Biol is available at www.ahajournals.org/journal/atvb

Nonstandard Abbreviations and Acronyms

H&E	hematoxylin and eosin Y
TBR	target to background ratio
VK	Von Kossa

macrophage activity, and plaque morphology with ^{18}F-NaF PET activity remains relatively unknown. This study aimed at investigating the correlates of ^{18}F-NaF PET activity against the histopathologic gold standard in ex vivo human coronary arteries. We hypothesize that ^{18}F-NaF PET activity would identify high-risk plaque via detection of microcalcification with and without the presence of lower-risk macrocalcification, advanced plaque morphology, and macrophage burden.

Highlights

- This study was performed to determine the correlation between ^{18}F-NaF activity and microcalcification in human coronary arteries.
- The current investigation demonstrated that high ^{18}F-NaF activity was associated with microcalcification in the coronary arteries, a feature of vulnerable plaque.
- High ^{18}F-NaF activity was also noted in the presence of advanced plaque morphology characterized by fibroatheromas, a feature of vulnerable plaque.
- Lower ^{18}F-NaF activity was associated with plaque without microcalcification or only macrocalcification and early plaque morphology characterized by intimal thickening.
- ^{18}F-NaF PET/CT of the coronary arteries has the potential to improve risk-stratification of atherosclerotic plaque.

MATERIALS AND METHODS

The authors declare that all supporting data are available within the article.

Specimen Selection

In this prospective cross-sectional study, we performed ^{18}F-NaF PET/CT on ex vivo coronary arteries from 9 deidentified patients who had undergone autopsy at Weill Cornell Medicine between 2015 and 2016. There were no prespecified exclusion criteria. This study was exempt from review by the local Institutional Review Board as it involved autopsy material, and no identifying information including clinical history was collected.

Two coronary artery samples were obtained per patient with the left main, left anterior descending, and left circumflex arteries as one specimen and the right coronary artery as the second specimen. Coronary artery specimens were obtained at the time of autopsy and placed in 4% formalin. A total of 18 coronary arteries were collected and imaged with ^{18}F-NaF PET/CT (Figure 1). One coronary artery was excluded due to technical difficulty in identifying which segments to slice by the pathologist as the coronary artery specimen changed in gross morphology after the PET/CT scan.

A total of 191 plaques from 17 coronary arteries were selected of which 90 plaques were subsequently excluded due to contamination of slides with calcified particles during the slicing process. A total of 101 coregistered plaques underwent histological analysis. Twenty-seven plaques were stained with hematoxylin and eosin Y (H&E), Von Kossa (VK), and CD68. Forty-three plaques were stained with H&E and VK, and 31 plaques were stained with H&E and CD68 without VK due to decalcification of the specimen during sample preparation. Slides prepared with EXAKT technology left an inadequate amount of tissue for staining with CD68.

Ex Vivo PET/CT Imaging

Coronary samples were immersed in ^{18}F-NaF (NCM USA, NY) solution diluted with PBS to a total activity of 0.37 MBq/mL (Life Technologies; Carlsbad, CA). After 60 minutes, coronary artery specimens were rinsed 3× in PBS before being placed into either a micro or clinical PET/CT scanner. The choice of scanner depended on availability.

A small animal micro-PET/CT system (Inveon, Siemens Medical Solutions) was used for imaging 14 coronary arteries. PET scan parameters were as follows: 5 minute acquisition/bed position, total 2 bed positions, 16 detector blocks (20×20 array of 1.5×1.5×10 mm lutetium oxyorthosciilicate crystal), total of 64 detectors, 12.7 cm axial and 10 cm transaxial field of view, and 3 dimensional OSEM-MAP (ordered subsets expectation maximization-maximum a posteriori) reconstruction algorithm. CT scan parameters were as follows: 165 mm, 10×10 cm (4064×4064 pixels) field of view, 80 kVP, 0.5 mA, and 196 µm resolution.

An integrated clinical PET/CT system (Biograph TruePoint PET/CT, Siemens Medical Solutions) was used to image 4 coronary arteries. PET scan parameters were as follows: 20 minute acquisition/bed position, total 1 bed position, 3D mode, 3 rings of 48 detectors blocks, 13×13 lutetium oxyorthosciilicate crystals (4×4×20 mm), 4 photomultiplier tubes, 163 mm field of view, 2 mm slice thickness, and 3D OSEM reconstruction algorithm. CT scan parameters were as follows: 16-slice helical CT (Somatom Sensation 16; Siemens Medical Solutions), 78 cm aperture, 2 mm slice thickness, minimum rotation time 0.3 seconds per 360°, maximum scan time per spiral 80 seconds, 140 kVP, 20 to 800 mA, and 0.24 mm reconstructed spatial resolution.

Image/Pathology Interpretation and Data Analysis

PET and CT scans were analyzed by an experienced nuclear medicine radiologist (T. Youn). Images were read and analyzed using advanced PET/CT review software (Inveon Research Workplace 4.2, Siemens Medical Solutions), which allowed analysis of PET, CT and fusion images in transverse, coronal, and sagittal planes with 3D visualization.

Regions of interest were selected if the arterial segment exhibited (1) focally increased ^{18}F-NaF activity with calcification on CT (PET+/CT+), (2) focally increased ^{18}F-NaF activity without calcification on CT (PET+/CT−), (3) no significant ^{18}F-NaF activity with calcification on CT or (PET−/CT+), and (4) no significant

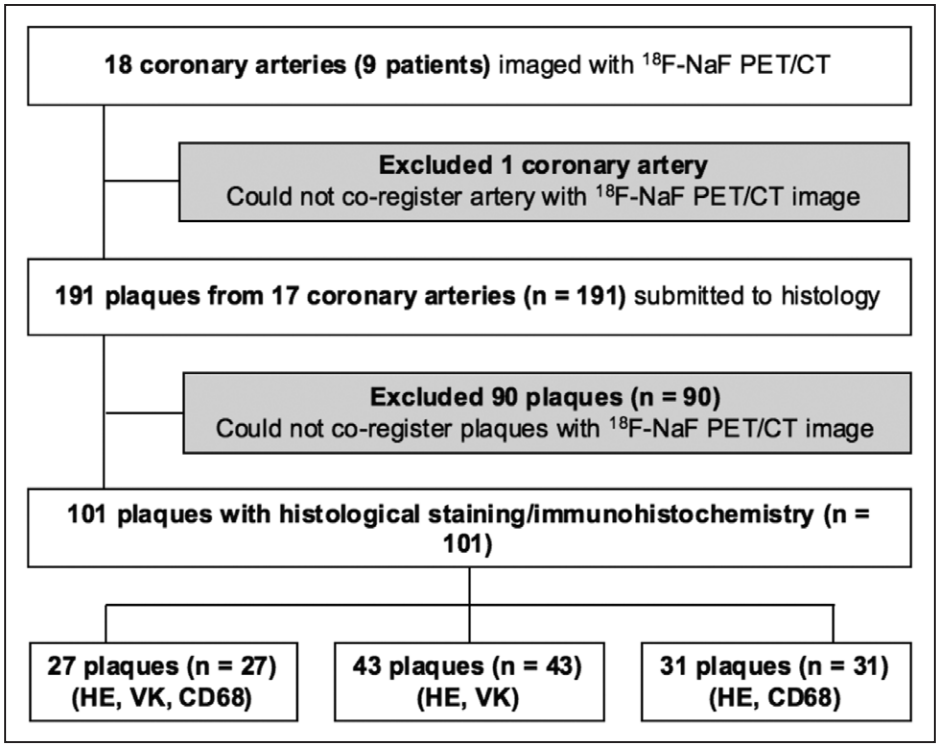

Figure 1. Flow diagram depicting the study design.
A total of 101 coregistered plaques underwent histological analysis. Twenty-seven plaques were stained with hematoxylin and eosin Y (H&E), Von Kossa (VK), and CD68. Forty-three plaques were stained with H&E and VK without CD68 due to scarcity of tissue, and 31 plaques were stained with H&E and CD68 without VK due to decalcification of the specimen during sample preparation.

^{18}F-NaF activity or calcification on CT (PET−/CT−). Increased ^{18}F-NaF activity was defined as visually assessed activity above background. No significant ^{18}F-NaF activity was defined as visually assessed activity similar to or below background. Regions of interest were drawn using transverse, coronal, sagittal, and 3D PET images for anatomic guidance. ^{18}F-NaF PET activity for each arterial segment was quantified using the target to background ratio (TBR) which was generated as follows: maximum counts on ^{18}F-NaF PET images in the region of interest divided by the maximum counts on ^{18}F-NaF PET images in the region of interest without significant ^{18}F-NaF activity or calcification on CT.

Histology/Immunohistochemistry and Data Analysis

After PET scanning, coronary artery specimens were sectioned based on coregistration with regions of interest chosen with ^{18}F-NaF PET/CT imaging. Radiographs were performed for further guidance if necessary. Severely calcified coronary specimens were processed based on a protocol at the CVpath institute using the EXAKT cutting and grinding system (EXAKT Technologies, Inc). Specimens were embedded in methylmethacrylate after dehydration in graded series of alcohol, sawed at 4 mm intervals, ground by EXAKT method between 70 and 120 microns, and stained with toluidine blue. Arteries with moderate calcification were decalcified in EDTA, whereas those with mild calcification were directly, without decalcification sectioned between 4 and 6 microns. Slides were subsequently stained with H&E and VK to detect calcification. They also underwent immunohistochemical staining for CD68 expression (mouse anti-human CD68 mAb, M0876, Dako) on a Leica Bond system using the standard protocol F. The section was pretreated using heat mediated antigen retrieval with sodium citrate buffer (pH 6, epitope retrieval solution 1) for 30 minutes. The section was then incubated with Agilent antibody (Catalog: M081401-2, 1:4000 dilution) for 15 minutes at room temperature and detected using a horseradish peroxidase conjugated compact polymer system. DAB (3,3′-diaminobenzidine) was used as the chromogen. The section was then counterstained with hematoxylin and mounted with Leica Micromount.

Histological slides were analyzed by an experienced pathologist (N. Narula). Microcalcification was defined as 0.5 to 15 μm in diameter, and macrocalcification was defined as calcification >15 μm in diameter. Calcification was evaluated on sections stained with H&E and VK. The primary outcome was the binary presence or absence of microcalcification on histopathology. Plaques with microcalcification included plaques with only microcalcification as well as plaques with both microcalcification and macrocalcification. Plaques without microcalcification included plaques with only macrocalcification and plaques without calcification. Atherosclerotic plaques were classified according to the modified American Heart Association classification into adaptive intimal thickening, pathological intimal thickening and fibroatheroma, as evaluated with H&E stained sections. The number of macrophages as assessed by immunohistochemical stain for CD68 were graded as follows: grade 0: a group comprising ≤5 cells; grade 1: a group between 6 and 50 cells or >1 group of <5 cells; grade 2: 2 to 5 groups of 6 to 50 cells; and grade 3: >5 groups of <50 cells or >1 group of >50 cells.[11]

Arterioscler Thromb Vasc Biol. 2020;40:404–411. DOI: 10.1161/ATVBAHA.119.312737

Statistical Analysis

^{18}F-NaF activity quantified by mean TBR was compared across groups. Larger mean TBR represented higher ^{18}F-NaF activity. The ANOVA test was used to compare plaques with different calcification, plaque morphology, and CD68 staining. The Tukey Honest Significance test was used to compare any 2 CD68 subgroups. The generalized estimating equation with adjustment of patient-level effect was performed on the log-transformed mean TBR, and exchangeable correlation structure was used in generalized estimating equation modeling. A 2-sided *P* value of <0.05 was considered statistically significant. Statistical analysis was performed using R (version 3.5.2 [2018-12-20]) and Stata 14 (StataCorp LP. College Station, TX).

RESULTS

Comparison of ^{18}F-NaF Activity in Plaques With and Without Microcalcification

We evaluated 101 plaques in 17 coronary arteries from 9 patients (Table and Figures 2 and 3). Eighty-four (83.2%) plaques demonstrated microcalcification and included 43 (42.6%) plaques with both microcalcification and macrocalcification and 41 (40.6%) plaques with only microcalcification. Seventeen (16.8%) plaques did not demonstrate microcalcification and included 2 (2.0%) plaques with only macrocalcification and 15 (14.9%) plaques without calcification.

Table. ^{18}F-Sodium Fluoride Positron Emission Tomography Activity in Plaques Categorized by the Presence of Microcalcification, Subgroups of Calcification, Plaque Grade, and Grade of CD68 Staining

	Mean TBR (SD)	Number (n=101)	*P* Values
Microcalcification (Y/N)			
Microcalcification	9.0 (9.7)	84	<0.0001*†
No microcalcification	2.9 (3.8)	17	
Subgroups of calcification			
No calcification	3.1 (4.1)	15	0.01*†
Only microcalcification	6.9 (9.5)	41	
Microcalcification/macrocalcification	11.1 (9.6)	43	
Only macrocalcification	1.8 (0.4)	2	
Plaque grade			
Fibroatheroma	10.7 (10.3)	54	0.004*†
Pathological intimal thickening	6.1 (8.4)	25	
Intimal thickening	3.5 (3.9)	22	
Grade of CD68 staining			
Grade 0 CD68 staining	3.2 (3.4)	22	0.08*†
Grade 1 CD68 staining	4.8 (5.6)	7	
Grade 2 CD68 staining	4.9 (3.7)	7	
Grade 3 CD68 staining	10.4 (14.1)	22	
Missing staining from lack of tissue	10.3 (8.3)	43	

TBR indicates target to background ratio.
*ANOVA test.
†*P* value significant if <0.05.

Plaques with microcalcification demonstrated higher ^{18}F-NaF activity (mean TBR±SD, 9.0±9.7) than plaques without microcalcification (mean TBR±SD, 2.9±3.8; *P*<0.0001). Regression analysis found plaques with microcalcification demonstrated 2.8× higher mean TBR (95% CI, 2.4–3.4; *P*<0.0001) than plaques without microcalcification.

Comparison of ^{18}F-NaF Activity Between Plaques With Different Types of Calcification

A significant difference in mean TBR was found between plaques without calcification (mean TBR±SD, 3.1±4,1), only microcalcification (mean TBR±SD, 6.9±9.5), both microcalcification and macrocalcification (mean TBR±SD, 11.1±9.6) and only macrocalcification (mean TBR±SD, 1.8±0.4, *P*=0.01) using ANOVA (Table and Figure 3). Plaques with only microcalcification demonstrated 2.0× higher mean TBR than plaques without calcification (95% CI, 1.7–2.3; *P*<0.0001). Plaques with both microcalcification and macrocalcification demonstrated 2.7× higher mean TBR than plaques with only macrocalcification (95% CI, 1.8–3.9; *P*<0.001). Using generalized estimating equation, no significant difference in ^{18}F-NaF activity was found between plaques without calcification and plaques with only macrocalcification (*P*=0.9). Additionally, no significant difference in ^{18}F-NaF activity was found between plaques with both microcalcification and macrocalcification and plaques with only microcalcification (*P*=0.9).

Comparison of ^{18}F-NaF Activity in Plaques With Different Plaque Morphology

Plaque morphology, from early to more advanced stages, was classified as fibroatheroma in 54 plaques (53.5%), pathological intimal thickening in 25 plaques (24.8%), and intimal thickening in 22 plaques (21.8%; Table and Figure 3).

Coronary fibroatheromas demonstrated higher ^{18}F-NaF activity (mean TBR±SD, 10.7±10.3) compared with plaques with less advanced plaque morphology, including intimal thickening (mean TBR±SD, 3.5±3.9) and pathological intimal thickening (mean TBR±SD, 6.1±8.4; *P*=0.004).

Comparison of ^{18}F-NaF Activity in Plaques With Different Degrees of CD68 Staining

CD68 staining, a marker of macrophages and inflammatory burden, was classified grade 0 in 22 plaques (37.9%), grade 1 in 7 plaques (12.1%), grade 2 in 7 plaques (12.1%), and grade 3 in 22 plaques (37.9%; Table).

Although not statistically significant (*P*=0.08), plaques with higher degrees of CD68 staining generally demonstrated higher ^{18}F-NaF activity compared with plaques with lower degrees of CD68 staining. Plaques with grade 3 CD68 staining had higher ^{18}F-NaF activity (mean TBR±SD,

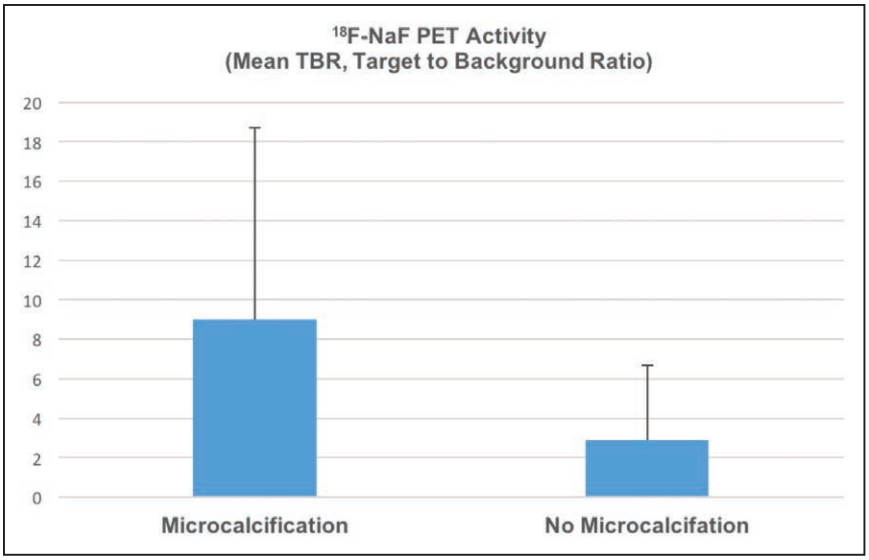

Figure 2. Higher ^{18}F-sodium fluoride (NaF) positron emission tomography (PET) activity is seen in plaque with microcalcification (mean target to background ratio [TBR]±SD, 9.0±9.7) compared with plaque without microcalcification (mean TBR±SD, 2.9±3.8).

10.4±14.1) compared with plaques with grade 0 CD68 staining (mean TBR±SD, 3.2±3.4), plaques with grade 1 CD68 staining (mean TBR±SD, 4.8±5.6), and plaques with grade 2 CD68 staining (mean TBR±SD, 4.9±3.7). Plaques in which CD68 staining could not be performed due to lack of tissue as noted in the methods section, demonstrated high ^{18}F-NaF activity (mean TBR±SD, 10.3±8.3). No significance was found in adjusted *P* values comparing any 2 CD68 subgroups. Statistical comparisons of the association between TBR and grades of CD68 staining may have been underpowered due to the small sample size.

DISCUSSION

In this study, we demonstrated in ex vivo human coronary artery plaques that higher ^{18}F-NaF activity is observed in plaques with microcalcification compared with those without microcalcification. ^{18}F-NaF detects calcification by irreversibly binding to hydroxyapatite in calcification.[7] Electron microscopy has demonstrated colocalization of fluoride to arterial calcification.[4] Given that microcalcification is a marker of high-risk coronary plaque, cannot be detected by conventional CT[4,6] and is masked on CT imaging by the presence of macrocalcification, ^{18}F-NaF PET/CT could be a useful noninvasive method to detect vulnerable plaque.

The current investigation demonstrated that higher ^{18}F-NaF activity was associated with features of vulnerable plaque including the presence of microcalcification, either with or without macrocalcification and advanced plaque morphology characterized by fibroatheromas (Figure 3). Similar to findings from carotid artery specimen examined by Irkle et al,[4] we also did not find an association with inflammation and ^{18}F-NaF activity in the coronary arteries. However, this may be due to the small sample size. Lower ^{18}F-NaF activity was associated with the lack of calcification or only macrocalcification and early plaque morphology characterized by intimal thickening (Figure 3). Plaques in which CD68 staining could not be performed due to difficulty sectioning heavy calcification, demonstrated high ^{18}F-NaF activity. There is a possibility that these excluded samples contained arterial segments with both microcalcification and macrocalcification, hence demonstrating high ^{18}F-NaF activity. However, further studies are needed to evaluate this hypothesis.

This study demonstrates correlation of ^{18}F-NaF PET/CT imaging with histology in the coronary arteries. In the carotid arteries, prior studies demonstrated ^{18}F-NaF PET activity co-localized with calcification on CT and ruptured plaque.[12,13] ^{18}F-NaF PET activity was also found to have a positive correlation with markers of active calcification, macrophage infiltration, apoptosis, and necrosis seen in endarterectomy specimen.[12] ^{18}F-NaF activity correlated with intravascular ultrasound findings of high-risk plaque, which include spotty calcification, positive remodeling, and necrotic core.[12] Furthermore, ^{18}F-NaF activity was highest in angiographically determined culprit lesions compared with nonculprit lesions.[12] Finally, ^{18}F-NaF activity in the coronary arteries correlated with prevalent cardiovascular risk factors such as older age, male sex, higher coronary calcium scores, and Framingham risk scores.[8]

Coronary heart disease is a major cause of morbidity and mortality worldwide and is prevalent in both males and females.[14] Current clinical practice has focused on the development of risk scores and predictive models that would risk-stratify individuals, with the hope of preventing adverse cardiovascular events in the highest risk group, albeit with limited accuracy. Noninvasive imaging, which uses computed tomography, has been geared towards coronary luminal evaluation and characterization of atherosclerotic plaque. Although CT can provide information on the presence of high-risk plaque features, the ability to predict culprit lesions in incident acute coronary events is limited. Molecular coronary

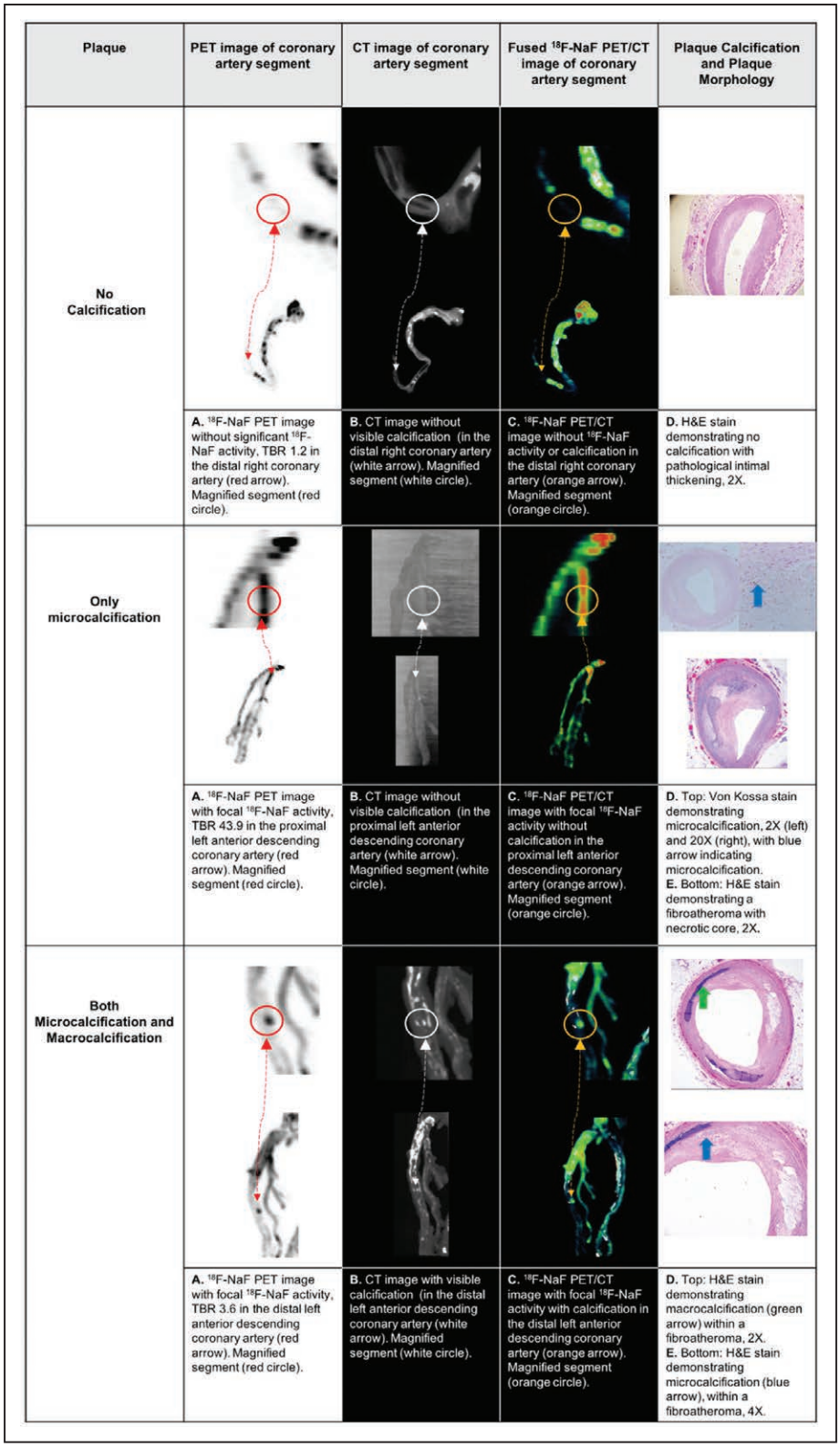

Figure 3. Chart demonstrating ^{18}F-sodium fluoride (NaF) positron emission tomography (PET) image, CT image, fused ^{18}F-NaF PET/CT image, and histology of plaques without calcification, only microcalcification or both microcalcification and macrocalcification.
H&E indicates hematoxylin and eosin Y; and TBR, target to background ratio.

imaging has been touted as the future of atherosclerosis evaluation and prognostication. Although correlating to macrophage infiltration in the carotid arteries,[15] ^{18}F-fluorodeoxyglucose PET/CT has a limited role for the evaluation of high-risk plaque in the coronary arteries due to adjacent physiological activity in the

myocardium.[8,12,16] However, our study indicates that there is potential for improvement in risk-stratification of individual plaque with ^{18}F-NaF PET/CT imaging which is not hindered by physiological activity within the myocardium.

This study also demonstrates that microcalcification and high ^{18}F-NaF activity likely indicates an active calcification process while macrocalcification and low ^{18}F-NaF activity may indicate advanced calcification and healed plaque. Microcalcification, measuring 0.5 to 15 µm in diameter, results from the formation of hydroxyapatite crystals after apoptosis of smooth muscle cells, or may result from matrix vesicles released by macrophages. Intimal microcalcification has been associated with high-risk plaque.[2,17] This idea that microcalcification is an active process, and macrocalcification is a healed stage was supported in earlier studies. ^{18}F-NaF activity was seen in areas of the coronaries without CT and intravascular ultrasound verified calcification, and ^{18}F-NaF activity was also seen in areas of the aortic valve without calcification that later developed macrocalcification on CT.[8,18] Presumably in these studies, the areas ^{18}F-NaF activity without calcification likely had microcalcification which healed and led to macrocalcification. On electron microprobe analysis, increased fluoride was seen in microcalcification compared with macrocalcification. In carotid arteries, ^{18}F-NaF activity localized to the surface of macrocalcification, as ^{18}F-NaF could not penetrate its core, leading to lower activity in plaques with macrocalcification than with plaques with microcalcification.[4] ^{18}F-NaF activity has been found to correlate with hydroxyapatite expression, which is likely higher in concentration within microcalcification compared with within macrocalcification, and not to overall extent of calcification.[19]

Furthermore, ^{18}F-NaF activity was not elevated in 41% of patients with coronary calcium scores >1000[8], indicating the presence of macrocalcification. Previously, ^{18}F-NaF activity inversely correlated with calcium density in coronary lesions in individuals with malignancies, where ^{18}F-NaF activity was highest in plaques without CT evidence of calcification or low CT density.[20]

Limitations of the Study

There were several limitations to the study. First, it was technically challenging to section selected plaques using ^{18}F-NaF imaging as guidance. As a result, one coronary artery and 90 plaques were excluded from analysis due to difficulties with correlation to the ^{18}F-NaF PET/CT images. Furthermore, relatively few plaques without significant ^{18}F-NaF activity were selected for evaluation, and as a result the investigation only included 2 plaques with macrocalcification for analysis. Second, heavily calcified arteries were difficult to section. During sectioning, many plaques were contaminated with calcified particles resulting in exclusion from analysis. Additionally, frequently there was an inadequate amount of tissue for staining with CD68. Decalcification of segments also left an inadequate amount of calcium for staining with VK. Given that the specimen were obtained from random autopsies, our results may not be representative of the general population. No clinical history was collected to correlate with imaging and histological findings. Also, our results may not be consistent as 4 coronary arteries were imaged with a clinical PET/CT, and 14 coronary arteries were imaged with a micro-PET/CT. However, a prior study by Irkle et al[4] has found that ^{18}F-NaF PET/CT imaging of carotid arteries and correlative histological findings of calcification did not differ between a clinical PET and micro PET. ^{18}F-NaF PET activity was not specific for the detection of intimal calcification. One of the plaque demonstrated both intimal calcification as well as calcification of the internal elastic lamina, which correlated to ^{18}F-NaF PET activity. The study was also limited by small sample size, likely under powering the evaluation of the relationship between inflammation and calcification. Finally, quantitative analysis in addition to our qualitative analysis of the area of calcification and ^{18}F-NaF PET activity would have provided significant information.

Future Directions

Molecular imaging of the coronary arteries with ^{18}F-NaF PET/CT is a promising imaging modality for the detection of high-risk plaque.[21] ^{18}F-NaF activity has been shown to correlate with vulnerable plaque features including microcalcification, advanced plaque morphology, and inflammation. More specifically, ^{18}F-NaF PET/CT may be most useful in the detection of high-risk plaque and improved risk-stratification of individuals beyond what is currently available. Moving forward, ^{18}F-NaF PET/CT could be evaluated in the clinical setting, with imaging of in vivo coronary arteries and correlating imaging findings with clinical outcomes. Also, as the localization of the microcalcification of at least 5 µm to the fibrous cap has been found to be significant in predicting plaque rupture,[22,23] it will be interesting to evaluate this in detail. The localization of microcalcification and ^{18}F-NaF PET activity in relation to CD68 staining, and the quantitative evaluation of the area of microcalcification, inflammation, fibrosis with ^{18}F-NaF PET activity would also be important to evaluate in subsequent studies. ^{18}F-NaF PET/CT imaging has the potential to improve predictive models and may lead to significant reductions in the incidence of adverse events by streamlining of preventative therapies to the highest risk individuals.

ARTICLE INFORMATION

Received March 29, 2019; accepted November 27, 2019.

Affiliations

From the Department of Radiology (T.Y., S.J.A., J.K.M.), Dalio Institute of Cardiovascular Imaging (S.J.A., F.Y.L., Y.L., A.K., J.K.M.), and Department of Pathology (S.S., D.P.), Weill Cornell Medicine, NY; Department of Pathology, New York University Langone Medical Center (N.N.); British Heart Foundation Centre for Cardiovascular Science, University of Edinburgh, Scotland, United Kingdom (M.R.D.);

Division of Cardiology, Mount Sinai Hospital, New York (J.N.); and CVpath Institute, Gaithersburg, MD (R.V.).

Acknowledgments

We are grateful to Simon Morim, Nelsie Pastrano, and Bin He at the Citigroup Biomedical Imaging Center.

Sources of Funding

The work was supported by the Dalio Institute of Cardiovascular Imaging.

Disclosures

J.K. Min serves on the scientific advisory board of Arineta, on the speaker's bureau of GE Healthcare, and owns equity in Cleerly. The other authors report no conflicts.

Supplemental Materials

Major Resources Table.

REFERENCES

1. Damen JA, Hooft L, Schuit E, Debray TP, Collins GS, Tzoulaki I, Lassale CM, Siontis GC, Chiocchia V, Roberts C, et al. Prediction models for cardiovascular disease risk in the general population: systematic review. *BMJ*. 2016;353:i2416. doi: 10.1136/bmj.i2416
2. Motoyama S, Kondo T, Sarai M, Sugiura A, Harigaya H, Sato T, Inoue K, Okumura M, Ishii J, Anno H, et al. Multislice computed tomographic characteristics of coronary lesions in acute coronary syndromes. *J Am Coll Cardiol*. 2007;50:319–326. doi: 10.1016/j.jacc.2007.03.044
3. Motoyama S, Sarai M, Harigaya H, Anno H, Inoue K, Hara T, Naruse H, Ishii J, Hishida H, Wong ND, et al. Computed tomographic angiography characteristics of atherosclerotic plaques subsequently resulting in acute coronary syndrome. *J Am Coll Cardiol*. 2009;54:49–57. doi: 10.1016/j.jacc.2009.02.068
4. Irkle A, Vesey AT, Lewis DY, Skepper JN, Bird JL, Dweck MR, Joshi FR, Gallagher FA, Warburton EA, Bennett MR, et al. Identifying active vascular microcalcification by (18)F-sodium fluoride positron emission tomography. *Nat Commun*. 2015;6:7495. doi: 10.1038/ncomms8495
5. Budoff MJ, Young R, Lopez VA, Kronmal RA, Nasir K, Blumenthal RS, Detrano RC, Bild DE, Guerci AD, Liu K, et al. Progression of coronary calcium and incident coronary heart disease events: MESA (Multi-Ethnic Study of Atherosclerosis). *J Am Coll Cardiol*. 2013;61:1231–1239. doi: 10.1016/j.jacc.2012.12.035
6. Otsuka F, Sakakura K, Yahagi K, Joner M, Virmani R. Has our understanding of calcification in human coronary atherosclerosis progressed? *Arterioscler Thromb Vasc Biol*. 2014;34:724–736. doi: 10.1161/ATVBAHA.113.302642
7. Czernin J, Satyamurthy N, Schiepers C. Molecular mechanisms of bone 18F-NaF deposition. *J Nucl Med*. 2010;51:1826–1829. doi: 10.2967/jnumed.110.077933
8. Dweck MR, Chow MW, Joshi NV, Williams MC, Jones C, Fletcher AM, Richardson H, White A, McKillop G, van Beek EJ, et al. Coronary arterial 18F-sodium fluoride uptake: a novel marker of plaque biology. *J Am Coll Cardiol*. 2012;59:1539–1548. doi: 10.1016/j.jacc.2011.12.037
9. Dweck MR, Doris MK, Motwani M, Adamson PD, Slomka P, Dey D, Fayad ZA, Newby DE, Berman D. Imaging of coronary atherosclerosis - evolution towards new treatment strategies. *Nat Rev Cardiol*. 2016;13:533–548. doi: 10.1038/nrcardio.2016.79
10. Creager MD, Hohl T, Hutcheson JD, Moss AJ, Schlotter F, Blaser MC, Park MA, Lee LH, Singh SA, Alcaide-Corral CJ, et al. 18F-Fluoride signal amplification identifies microcalcifications associated with atherosclerotic plaque instability in positron emission tomography/computed tomography images. *Circ Cardiovasc Imaging*. 2019;12:e007835. doi: 10.1161/CIRCIMAGING.118.007835
11. Virmani R, Kolodgie FD, Burke AP, Farb A, Schwartz SM. Lessons from sudden coronary death: a comprehensive morphological classification scheme for atherosclerotic lesions. *Arterioscler Thromb Vasc Biol*. 2000;20:1262–1275. doi: 10.1161/01.atv.20.5.1262
12. Joshi NV, Vesey AT, Williams MC, Shah AS, Calvert PA, Craighead FH, Yeoh SE, Wallace W, Salter D, Fletcher AM, et al. 18F-fluoride positron emission tomography for identification of ruptured and high-risk coronary atherosclerotic plaques: a prospective clinical trial. *Lancet*. 2014;383:705–713. doi: 10.1016/S0140-6736(13)61754-7
13. Derlin T, Tóth Z, Papp L, Wisotzki C, Apostolova I, Habermann CR, Mester J, Klutmann S. Correlation of inflammation assessed by 18F-FDG PET, active mineral deposition assessed by 18F-fluoride PET, and vascular calcification in atherosclerotic plaque: a dual-tracer PET/CT study. *J Nucl Med*. 2011;52:1020–1027. doi: 10.2967/jnumed.111.087452
14. Mozaffarian D, Benjamin EJ, Go AS, Arnett DK, Blaha MJ, Cushman M, Das SR, de Ferranti S, Després JP, Fullerton HJ, et al; Writing Group Members. Heart disease and stroke statistics-2016 update: a report from the American Heart Association. *Circulation*. 2016;133:e38–360. doi: 10.1161/CIR.0000000000000350
15. Cocker MS, Spence JD, Hammond R, deKemp RA, Lum C, Wells G, Bernick J, Hill A, Nagpal S, Stotts G, et al; Canadian Atherosclerosis Imaging Network (CAIN) - Project II. [18F]-Fluorodeoxyglucose PET/CT imaging as a marker of carotid plaque inflammation: comparison to immunohistology and relationship to acuity of events. *Int J Cardiol*. 2018;271:378–386. doi: 10.1016/j.ijcard.2018.05.057
16. Rudd JH, Warburton EA, Fryer TD, Jones HA, Clark JC, Antoun N, Johnström P, Davenport AP, Kirkpatrick PJ, Arch BN, et al. Imaging atherosclerotic plaque inflammation with [18F]-fluorodeoxyglucose positron emission tomography. *Circulation*. 2002;105:2708–2711. doi: 10.1161/01.cir.0000020548.60110.76
17. Ehara S, Kobayashi Y, Yoshiyama M, Shimada K, Shimada Y, Fukuda D, Nakamura Y, Yamashita H, Yamagishi H, Takeuchi K, et al. Spotty calcification typifies the culprit plaque in patients with acute myocardial infarction: an intravascular ultrasound study. *Circulation*. 2004;110:3424–3429. doi: 10.1161/01.CIR.0000148131.41425.E9
18. Dweck MR, Jenkins WS, Vesey AT, Pringle MA, Chin CW, Malley TS, Cowie WJ, Tsampasian V, Richardson H, Fletcher A, et al. 18F-sodium fluoride uptake is a marker of active calcification and disease progression in patients with aortic stenosis. *Circ Cardiovasc Imaging*. 2014;7:371–378. doi: 10.1161/CIRCIMAGING.113.001508
19. Cocker MS, Spence JD, Hammond R, Wells G, deKemp RA, Lum C, Adeeko A, Yaffe MJ, Leung E, Hill A, et al. (CAIN) CAIN. *JACC Cardiovasc Imaging*. 2017;10:486–488.
20. Fiz F, Morbelli S, Piccardo A, Bauckneht M, Ferrarazzo G, Pestarino E, Cabria M, Democrito A, Riondato M, Villavecchia G, et al. ^{18}F-NaF uptake by atherosclerotic plaque on PET/CT imaging: inverse correlation between calcification density and mineral metabolic activity. *J Nucl Med*. 2015;56:1019–1023. doi: 10.2967/jnumed.115.154229
21. Doris MK, Newby DE. Identification of early vascular calcification with (18)F-sodium fluoride: potential clinical application. *Expert Rev Cardiovasc Ther*. 2016;14:691–701. doi: 10.1586/14779072.2016.1151354
22. Kelly-Arnold A, Maldonado N, Laudier D, Aikawa E, Cardoso L, Weinbaum S. Revised microcalcification hypothesis for fibrous cap rupture in human coronary arteries. *Proc Natl Acad Sci U S A*. 2013;110:10741–10746. doi: 10.1073/pnas.1308814110
23. Maldonado N, Kelly-Arnold A, Laudier D, Weinbaum S, Cardoso L. Imaging and analysis of microcalcifications and lipid/necrotic core calcification in fibrous cap atheroma. *Int J Cardiovasc Imaging*. 2015;31:1079–1087. doi: 10.1007/s10554-015-0650-x